

Multi-Domain Structural-Acoustic Coupling Analysis Using the Finite Element and Boundary Element Techniques

Hyeon-Don Ju*†

Graduate School, Department of Mechanical Design Engineering, Pusan National University

Shi-Bok Lee

School of Mechanical Engineering, Pusan National University

A new approach to analyze the multi-domain acoustic system divided and enclosed by flexible structures is presented in this paper. The boundary element formulation of the Helmholtz integral equation is used for the internal fields and the finite element formulation for the structures surrounding the fields. We developed a numerical analysis program for the structural-acoustic coupling problems of the multi-domain system, in which boundary conditions such as the continuity of normal particle velocity and sound pressure in the structural interfaces between Field 1 and Field 2 are not needed. The validity of the numerical analysis program is verified by comparing the numerical results with the experimental ones. Example problems are included to investigate the characteristics of the coupled multi-domain system.

Key Words : Structural-Acoustic Coupling, Multi-Domain Acoustic System, FEM (Finite Element Method), Direct BEM (Boundary Element Method)

1. Introduction

The surface vibration of structures causes most noise problems in the machinery such as aircraft, railway and automobile. Recent pursuit for economic structures with lesser weight and thickness has urged us to pay attention to the structural-acoustic coupling effect more seriously. According to this need, much effort has been poured into the coupled fluid-structure interaction analysis, especially for the cavity in railway, automobile, aircraft, submerged structures and fluid-filled piping systems. For simple structures such as a membrane, plate, and cylindrical shell, the interaction problems between the structure and the acoustic media have been solved analytically

by approximate methods. On the other hand, numerical methods are widely adopted to treat the problems of complicated thin structures. The finite element method for most sound field analysis requires much more computing cost than the boundary element method. The Direct BEM technique (Seybert and Cheng, 1987) and multi-domain BEM technique (Cheng and Seybert, 1991) were shown to be successful in determining the acoustic response of cavities and the transmission loss (TL) of muffler elements. The BEM for an impedance boundary condition makes it possible to treat the acoustic effect of absorbent materials pasted on vibrating structures (Suzuki, 1989). A large-scale structural-acoustic uncoupled method has been used to calculate the BEM matrix of each field in several acoustic fields and to solve the global BEM matrix simultaneously for all of the boundary unknowns (Koki et al., 1998). Light structures may be influenced by the mass and/or the damping provided by the surrounding fluid. These coupled structural/acoustic problems can be solved simultaneously by the finite element and boundary element

† First Author

* Corresponding Author,

E-mail : hdju2433@hanmail.net

TEL : +82-55-751-8149; FAX : +82-55-761-7407

Graduate School, Department of Mechanical Design Engineering, Pusan National University, Pusan 609-735, Korea. (Manuscript Received June 7, 2000 ; Revised February 5, 2001)

techniques. It is, however, impossible to analyze the sound transmission through thin elastic plates in architectural acoustics, machine cavity design, silencer design, and underwater acoustics by one acoustic field analysis.

A multi-domain boundary element technique for a two-field, three-domain, fluid-structure-fluid interaction problem has been developed (Wu and Dandapani, 1994). There, the continuity of normal velocity was adopted as the interface condition for the thin-walled interface structure. But this interface condition cannot generally deal with the general multi-domain structural-acoustic system consisting of more than two acoustic fields.

This paper presents a new approach that can analyze the general coupled structural-acoustic multi-domain systems. A two-field duct divided and enclosed by flexible structures (see Fig. 1), which is a structure-fluid-structure-fluid-structure system, is introduced to numerically determine two-way coupling effects between the internal fluids and structures. We divide the boundary structure S into four parts (S_1 , S_2 , S_3 , and S_4). S_1 and S_4 are the outer structures enveloping the two intact fields, and S_2 , S_3 are the structural interfaces between the two fields. All boundaries are constructed by thin elastic plates. The boundary element formulation of the Helmholtz integral equation is used for the internal fields and the finite element formulation is used for the structures surrounding the fields. Interface conditions such as the continuity of normal particle velocity and the continuity of sound pressure are not needed. Both the vibration of structures and the internal sound pressures of the two fields are computed to especially consider the two-way coupling effects. Experimental results are compared with the numerical solutions for verifying the effectiveness of the developed program. Finally, numerical examples are considered to investigate the characteristics of the coupled multi-domain system, varying the size and internal fluids of the cavities.

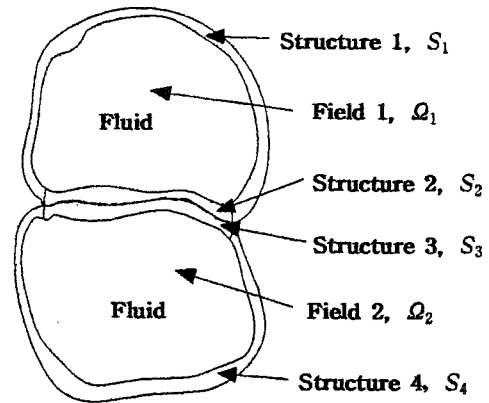


Fig. 1 Schematic diagram of two-field system

2. Modeling and Analysis of Coupled Structural-Acoustic Multi-Domain System

A three-dimensional cavity enclosed by a surface structure can be divided into several cavities to yield a multi-domain problem. The boundary integral formulation for the problem can be explained by considering a three-dimensional enclosed structure with only two fields, Ω_1 and Ω_2 separated by interface structures, S_2 and S_3 as illustrated in Fig. 1. The boundary surface is divided into four parts, i.e. S_1 , S_2 , S_3 , and S_4 . Fluids in Ω_1 and Ω_2 are treated as compressible, inviscid, nonflowing fluid media. For time-harmonic excitation, the velocity potential in the fluids must satisfy the Helmholtz equation.

$$\nabla^2 \phi + k^2 \phi = 0, \quad k = \omega / c \quad (1)$$

where ∇^2 is the Laplacian operator, ϕ is the velocity potential of the field, and k , c and ω are the wave number, sound speed, and angular frequency, respectively. The normal particle velocity of the fluid at the boundary surfaces is $u = \frac{\partial \phi}{\partial n}$ where $\partial/\partial n$ is the normal derivative, n is the unit normal on the boundary surface of a field, S , directed away from the volume of the field, Ω . Sound pressure in the field can be calculated by $p = -j\omega\rho_0\phi$, where $j = \sqrt{-1}$ and ρ_0 is the fluid density. Eq. (1) can be transformed into the integral equation as follows:

$$C^0(p)\phi(p) = \int_s \{ \psi(P, Q) \frac{\partial \phi}{\partial n}(Q) - \phi(Q) \frac{\partial \psi}{\partial n}(P, Q) \} dS(Q) \quad (2a)$$

where P is a collocation point and Q is any field point on S .

The function ϕ is the three-dimensional free-field Green's function, $\psi(P, Q) = \exp[-ikR(P, Q)]/R(P, Q)$, in which $R(P, Q)$ is the distance between P and Q . The coefficient $C^0(P)$ has the value 4π for P in Ω , and on any arbitrary surface can be evaluated by the following equation (Seybert et al., 1985).

$$C^0(p) = - \int_s \frac{\partial}{\partial n} \left(\frac{1}{R(P, Q)} \right) dS(Q) \quad (2b)$$

The boundary surfaces are discretized by rectangular elements that have four nodes. If the collocation points are taken to the surface nodes, Eq. (2a) leads to the following discretized boundary integral equation:

$$\sum_{m=1}^N \sum_{a=1}^4 \phi'_{ma} \cdot a_{mj}^a - \sum_{m=1}^N \sum_{a=1}^4 \phi_{ma} \cdot b_{mj}^a = - \sum_{m=1}^N C_{mj} \cdot \phi_j \quad (j=1, 2, 3, n) \quad (3)$$

where N is the number of elements, j denotes the j -th collocation point, and n represents the number of nodes on the boundary surface. ϕ_{ma} and ϕ'_{ma} are, respectively, the velocity potential and the derivative of the potential of the a -th node of the m -th element in isoparametric coordinates r and s , and ϕ_j is the potential of the j -th collocation point at (r, s) . The influence coefficients are given as

$$a_{mj}^a = \int_{-1}^1 \int_{-1}^1 \frac{e^{-ikR_{mj}}}{R_{mj}} N_a(r, s) \cdot J_m(r, s) dr ds \quad (4a)$$

$$b_{mj}^a = \int_{-1}^1 \int_{-1}^1 \frac{\partial}{\partial n} \left(\frac{e^{-ikR_{mj}}}{R_{mj}} \right) N_a(r, s) \cdot J_m(r, s) dr ds \quad (4b)$$

$$C_{mj} = \int_{-1}^1 \int_{-1}^1 \frac{\partial}{\partial n} \left(\frac{1}{R_{mj}} \right) \cdot J_m(r, s) dr ds \quad (4c)$$

where $J_m(r, s)$ is the Jacobian isoparametric transformations, $N_a(r, s)$ is the shape function of the isoparametric co-ordinates (r, s) , and R_{mj} is the distance from the collocation point, j , to any surface point of the m -th element. Express ϕ_j as $\delta_{ji} \cdot p_i$ with δ_{ij} being the Kronecker delta and let

$$B_{ji} = \overline{B_{ji}} - \left(\sum_{m=1}^N C_{mj} \right) \delta_{ji} \quad (5)$$

Then, Eq. (3) becomes

$$\sum_{i=1}^M B_{ji} \cdot \phi_i = \sum_{i=1}^M A_{ji} \cdot \phi_i \quad (j=1, 2, 3, \dots, n) \quad (6)$$

where M is the number of nodes on the boundary surface. Substituting $\phi = p/(-j\omega \cdot \rho_0)$ and $\phi' = u$ into Eq. (6), we can obtain the equation

$$\sum_{i=1}^M \left(\frac{B_{ji}}{-i\omega\rho} \right) \cdot p_i = \sum_{i=1}^M A_{ji} \cdot u_i \quad (j=1, 2, \dots, M) \quad (7)$$

If either sound pressure p_i or sound particle velocity u_i is known at every point on the boundary, the other can readily be calculated from Eq. (7).

For structural analysis, four-node thin plate elements are adopted. If the rotational degrees of freedom are condensed out, the translational degrees of freedom are obtained. In addition, if the boundaries of the structure are either clamped or simply supported, the displacement on the boundary can be condensed out. The finite element equation of the structure is written as

$$(-\omega^2 M_s + K_s) x = f^{rad} + f_d \quad (8)$$

where K_s is the stiffness matrix, M_s is the mass matrix, x is the displacement vector, f^{rad} is the additional structural load created by the acoustic pressure on the structure, and f_d is the vector of structural forces applied. The additional structural load f^{rad} is computed as

$$f^{rad} = - \sum_m \sum_a c_{ma} \cdot p_{ma} = - \sum_i c_i \cdot p_i = - c^T \cdot p \quad (9)$$

where $c_{ma} = \int_{-1}^1 \int_{-1}^1 N_a(r, s) \cdot J_m(r, s) dr ds$, and c^T is the geometric coupling matrix between acoustic pressures and forces on the structure (Ciskowski and Brebbia, 1991).

The displacement vector is found from Eq. (8) as

$$x = -(-\omega^2 M_s + K_s)^{-1} c^T p + (-\omega^2 M_s + K_s)^{-1} f_d \quad (10)$$

In the two interior acoustic fields, combination of Eq. (7) and Eq. (8) results in the following matrix notation:

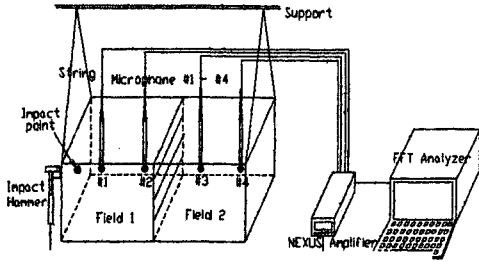


Fig. 2 Experimental setup

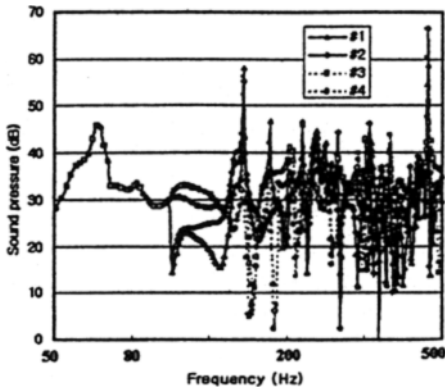


Fig. 3 Experimental frequency responses of sound pressure

$$\begin{pmatrix} (K_s - \omega^2 M_s)_I & c^T & (K_s - \omega^2 M_s)_S & 0 \\ \rho \cdot \omega^2 \cdot A(K)_I & B(K)_I & 0 & 0 \\ (K_s - \omega^2 M_s)_2 & 0 & (K_s - \omega^2 M_s)_{II} & c^T \\ 0 & 0 & \rho \cdot \omega^2 \cdot A(K)_{II} & B(K)_{II} \end{pmatrix} \cdot \begin{pmatrix} x_I \\ p_I \\ x_{II} \\ p_{II} \end{pmatrix} = \begin{pmatrix} f_{aI} \\ 0 \\ f_{aII} \\ 0 \end{pmatrix} \quad (11)$$

where the subscripts 1, 2, 3 and 4 denote quantities for $S_1, S_2, S_3,$ and S_4 in Fig. 1, respectively. The subscripts I and II denote the contribution from Ω_1 and $\Omega_2,$ respectively. Eq. (11) can be solved for all of the sound particle velocity and sound pressure unknowns on the surface of structures. If both the normal sound particle velocity and the sound pressure are known on S_1, S_2 (or S_3, S_4) in Fig. 1, sound pressures at any field point in the sub-field Ω_1 (or Ω_2) may be computed.

Table 1 Material properties of the structure and fluid

Parameter		Value
Fluid	Air	Density ρ / kg/d
		Velocity
Thickness		Outside : 0.002m Inside : 0.00025m
Plate	Young's modulus	
	Poisson's ratio	
	Density	

3. Experiments and Numerical Analysis

For the verification of the developed analysis program through comparisons between the numerical and experimental results, we constructed a steel parallelepiped with two cavities using thin surface plates and a thin inserted plate as shown in Fig. 2. The system represents a two-field structural-acoustic coupling problem. Each field has a size of 0.25 x 0.25 x 0.75m, and was divided into 256 four-node thin plate elements in the numerical modeling. The left end plate of the box in Field 1 was vibrated by an impact hammer to obtain the data over a broad band of frequency at a time. Sound pressure was measured at two positions per each field and compared. The locations of the 4 measuring points are 0.175m(#1), 0.375m(#2), 1.125m(#3), and 1.325m(#4), respectively, from the left end plate of Field 1. The boundaries of the enclosing structures were set free. Sound pressure levels were measured simultaneously using four microphones (B&K 4188) and analyzed using a B&K Pulse 3060 FFT Analyzer.

Table 1 presents the material properties of the structure and the fluid in the cavities. Figure 3 shows the frequency responses of sound pressure at the four measuring points.

The peaks at the frequencies of 65Hz, 154Hz, and 460Hz are due to the resonant modes of the side plate, the end plate and the cavity volume in each field, respectively. Figure 4 represents the numerical analysis results of the developed program. Figure 5 compares the numerical fre-

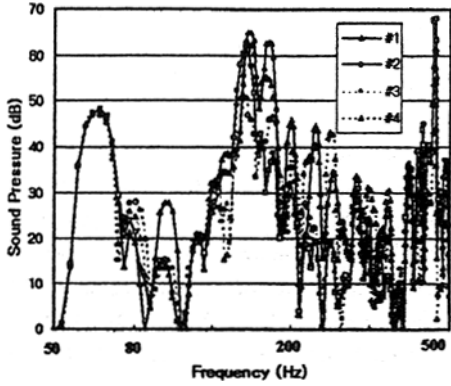
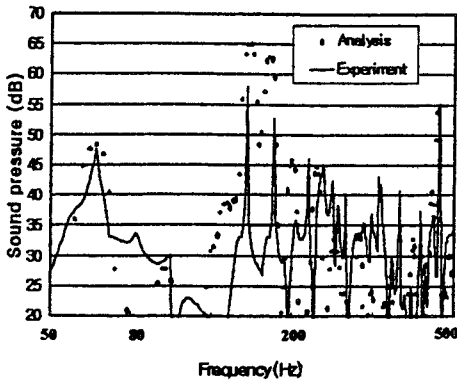
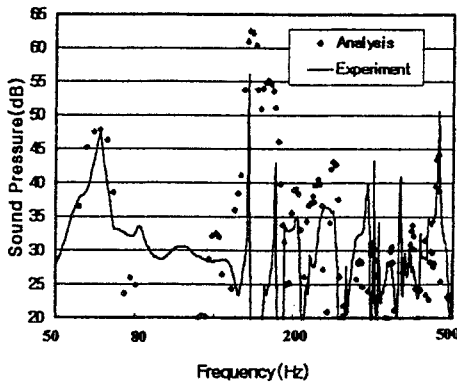


Fig. 4 Numerical frequency responses of sound pressure



(a) Point #1



(b) Point #4

Fig. 5 Comparison of experimental and simulation frequency response results

quency response results with the experimental ones at the first and fourth measuring points, respectively. It appears that the numerical results

Table 2 Material properties of the structure and fluids

Parameter		Value	
Fluid	Air	Density	1.21kg/m ³
		Velocity	346m/s
	Sea water	Density	1030kg/m ³
		Velocity	1500m/s
Plate	Thickness		0.001m
	Young's modulus		207GPa
	Poisson's ratio		0.3
	Density		7810kg/m ³

Table 3 Six simulation models

	Model					
	1	2	3	4	5	6
Field size (m×m×m)	3×3×3	3×3×3	3×3×6	3×3×6	3×3×7	3×3×7
No.of element	112	112	184	184	208	208
Fluid	sea water	air	sea water	air	sea water	air

Table 4 Overall SPLs at the measurement points for the six models [dB]

Field	Point	Model					
		1	2	3	4	5	6
1	1	99.7	43.8	107.6	50.3	103.4	43.4
	2	102.0	45.5	106.1	48.7	103.0	43.4
	3	104.6	48.0	105.2	46.0	101.9	42.7
	4	105.1	48.6	105.2	48.2	100.9	41.4
	5	104.3	47.1	106.6	50.0	100.1	40.0
2	1	101.0	45.2	104.3	45.4	107.4	45.6
	2	104.7	46.7	105.4	47.2	108.7	47.6
	3	103.8	45.5	109.0	50.4	115.0	49.4
	4	103.2	43.7	109.3	50.1	111.6	47.9
	5	99.5	40.6	107.2	45.3	110.6	45.8

are in good agreement with the experimental results. These comparison results clearly show the effectiveness and accuracy of our program for the multi-domain coupled structural-acoustic analysis.

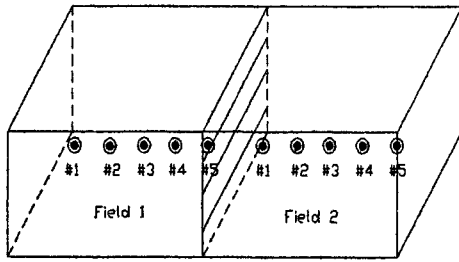
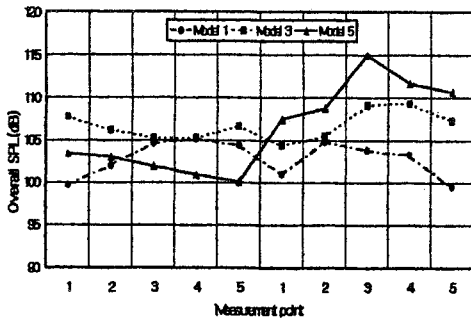
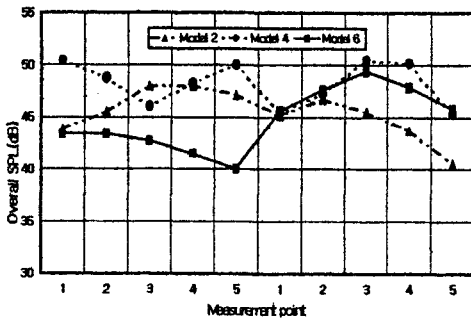


Fig. 6 Simulated points in each field



(a) Models 1, 3 and 5



(b) Models 2, 4 and 6

Fig. 7 SPLs at measurement points

4. Numerical Examples and Discussions

Here, we further go on to investigate the characteristics of the coupled multi-domain system using the developed program. Table 2 presents the material properties of the structure and inner fluids in the cavities. As shown in Table 3, six different models, which are discriminated by the inner fluids and the dimension of the fields, are simulated.

In order to simulate the fluid-structure

interaction, one of the two enclosing lateral faces of the cavities was harmonically excited to generate an acoustic disturbance. Table 4 presents the overall sound pressure levels (SPL) at all the simulated points in Fig. 6.

It appears in Fig. 7 that the SPLs of Models 1, 3, and 5 with sea water fluid are greater than those of Models 2, 4, and 6 with air fluid because the fluid-structure interaction effects in Models 1, 3, and 5 are greater than those of Models 2, 4, 6. Model 1 has the shortest (3m) cavity for each field and shows the standing-wave fluid resonance in both Fields 1 and 2. Model 5 has the longest (7m) cavity for each field and shows the standing wave resonance only in Field 2, but only the incident wave along the length direction in Field 1. The incident wave vibrates the interface structure. The sound pressure has a jump across the interface structure, and SPL in Field 2 increases. The higher SPLs in Field 2 of Model 5 than those of Model 1 result from the greater fluid mass.

5. Conclusions

We developed a numerical analysis program for the coupled structural-acoustic multi-domain problems using the finite element/boundary element method (FEM/BEM). For the verification of the program, the numerical and experimental analysis results for a prismatic coupled multi-domain system with two cubic cavities were compared. The frequency responses and overall levels of sound pressure in the cavities measured by experiments show reasonable agreement with the simulation. That confirms the effectiveness and accuracy of the developed program for the coupled structural-acoustic multi-domain analysis. Example problems were also considered to investigate the characteristics of the coupled multi-domain system.

References

Cheng, C.Y. R. and Seybert, A.F., 1991, "A Multi-Domain Boundary Element Solution for Silencer and Muffler Performance Prediction," *J. of Sound and Vibration*, Vol. 151, No. 1, pp. 119

~129.

Ciskowski, R. D. and Brebbia, C. A., 1991, *Boundary Element Methods in Acoustics*, Computational Mechanics Publications.

Fahy, F. J., 1985, *Sound and Structural Vibration*, Academic Press.

Hong, C. S., Shin, K. K., 1997, "Applications of General-Purpose Package for Fluid-structure Interaction Problems," *Journal of KSNVE*, Vol. 7, No. 4, pp. 571~578.

Kang, D. C., Ju, H.D. and Lee, S. B., 1999, "Multi-Domain Structural-Acoustic Coupling Analysis Using Finite Element and Boundary Element Technique," *Proceedings of the KSNVE, Fall Annual Meeting*, pp. 928~935.

Koki, Shiohata, Kanako, Nemoto and Takuzou, Iwatsubo, 1998, "A Large Scale Structural-Acoustic Analysis Method," *Journal of the JSME(C Part)*, Vol. 64, No. 622, pp. 125~130.

Lee, C. M., 1996, "Application of Finite Element and Boundary Element Methods to Predict Steady-State Response of a Structure-Acoustic-Cavity System," *Trans. of KSME(A Part)*, Vol. 20, No. 5, pp. 1383~1391.

Lee, D. I., Oh, J. E., 1996, "A Free Vibration

Analysis of Sound-Structure Interaction Plate," *Trans. of KSME(A Part)*, Vol. 20, No. 8, pp. 2546~2554.

Petyt, M., 1990, *Introduction to Finite Element Vibration Analysis*, Cambridge University Press.

Seybert, A. F., Soenarko, B. and Rizzo, F.J. and Shippy D. J., 1985, "Advanced Computational Method for Radiation and Scattering of Acoustic Waves in Three Dimensions," *J. Acoustical Society of America*, Vol. 77, No. 2, pp. 362~368.

Seybert, A.F. and Cheng, C. Y. R., 1987, "Application of the Boundary Element Method to Acoustic Cavity Response and Muffler Analysis," *J. of Vibration, Acoustics, Stress, and Reliability in Design*, Vol. 109, pp. 15~21.

Suzuki, S., 1989, "Boundary Element Analysis of Cavity Noise Problems with Complicated Boundary Conditions," *J. of Sound and Vibration*, Vol. 130, pp. 79~91.

Wu, T.W. and Dandapani, A., 1994, "A Boundary Element Solution for Sound Transmission Through Thin Panels," *J. of Sound and Vibration*, Vol. 171, No. 2, pp. 145~157.